

Mixed, charge and heat noises in thermoelectric nanosystems

Adeline Crépieux¹ and Fabienne Michelini²

¹*Aix Marseille Université, Université de Toulon,
CNRS, CPT UMR 7332, 13288 Marseille, France and*

²*Aix Marseille Université, CNRS, IM2NP, UMR 7334, 13288 Marseille, France*

Mixed, charge and heat zero-frequency noises, as well as thermoelectric differential conductances, are considered in non-interacting nanosystems connected to two reservoirs within the Landauer-Büttiker formalism. We introduce a dimensionless quantity given by the ratio between the product of mixed noises and the product of charge and heat noises, distinguishing between auto-ratios defined in the same reservoir and cross-ratios between distinct reservoirs. In the linear response regime, we find that these ratios are all equal to each other and coincide with the thermoelectric figure of merit. They are also simply related to the differential conductances since the latter quantities are related to noises by the fluctuation-dissipation theorem. In the non-linear regime, these ratios exhibit rich and complex behaviors related to properties of the noises, which encourages to deeper examine their possible connections to thermoelectric efficiency.

I. INTRODUCTION

The main motivation for studying thermoelectricity in quantum systems is the promise to increase the conversion efficiency by reducing the dimension. Indeed, the first measurements of values larger than one for the figure of merit were obtained in superlattices and quantum dot superlattices.^{1,2} These observations were the trigger signal of a large number of both experimental and theoretical works. Increase of the thermopower has been obtained in molecular junctions between a gold substrate and a gold scanning tunneling microscope tip,³ and measurements of Seebeck coefficient have been performed in carbon nanotubes,^{4,5} control break junctions,⁶ magnetic tunnel junctions,⁷ spin valves,⁸ and Kondo quantum dots.⁹ Non-linear thermovoltage and thermocurrent in quantum dot have also been highlighted.¹⁰

In parallel, extensive theoretical works were performed in order to understand how thermoelectric properties are affected in nanosystems with multi channels,¹¹ multi-terminals,¹² on-site interaction,^{13,14} inelastic scattering,^{15,16} and time-dependent voltage.^{17,18} Besides, the validity of the Onsager relation linking the Seebeck and Peltier coefficients, the validity of the Wiedemann-Franz and Fourier laws were also questioned in nanosystems.^{12,19–21} Indeed, the breakdown of thermoelectric reciprocity relations has been experimentally observed recently in a four-terminals mesoscopic device.²²

A key point for thermoelectricity in nanosystems is the fact that the tools used to quantify the efficiency for classical systems fail to describe the quantum ones. In particular, the figure of merit is a concept which makes sense only in the linear response regime. Indeed, the optimization of the figure of merit in nanosystems does not guarantee the optimization of the efficiency.²³ Thus, one has rather to consider directly the efficiency, and look for the optimization of the ratio between electrical and heat powers.^{24–26} Another witness of the thermoelectric conversion is the signal to noise ratio. The interest in heat noise in quantum systems and its relation to thermoelec-

tric conversion is currently growing up. However, these studies are mainly restricted to correlations between the heat current and itself.^{27–30} In particular, it has been shown that the correlator between heat currents in distinct reservoirs is not necessary positive contrary to what happens for charge currents.³¹ It is only recently that the correlation between heat and charge currents – that we call mixed noise – has been considered,³² and that a ratio between the different kinds of noises has been introduced.³³

In this work, we investigate the mixed, charge and heat noises in non-interacting nanoscopic systems connected to two reservoirs, drawing special attention to the ratio between the product of mixed noises and the product of charge and heat noises. From the Landauer-Büttiker formalism,³⁴ we derived analytical expressions of the noises, thermoelectric differential conductances and consider their possible relationships in the entire ranges of temperature, voltage and coupling to environment or reservoirs. In the extreme regimes of high temperature, which is linear, and high voltage, we further specify the expressions of differential conductances, noises and ratios, and examine their behavior in two concrete nanosystems: a quantum point contact (QPC) in an ohmic environment and a quantum dot (QD) with a single energy level.

In the linear response regime, we recover fluctuation-dissipation theorems which link the electrical and thermal conductances to the charge and heat noises. In addition, we find that the fluctuation-dissipation theorem also applies for mixed noises provided one considers the *new* thermoelectric conductances we have introduced. As a consequence, the figure of merit can be expressed as the ratio between the square of mixed noise and the product of heat and charge noises.

In the non-linear response regime with voltage, we were guided to distinguish between two ratios of noises: the cross-ratio that is defined between two different reservoirs and the auto-ratio defined inside the same reservoir. Significantly in the two nanosystems, the cross-ratio can reach larger values than one, while the auto-ratio cannot

exceed one. Similarly in between these two regimes, the cross-ratio reveals complex behavior that manifests features of the different noises and likely carry informations on thermoelectric conversion, to be further elucidate.

The paper is organized as follows: in Sec. II, we define all the quantities we are interested in, i.e. differential conductances, current noises at zero frequency and ratios of noises. We give the general expressions of these quantities obtained in the framework of Landauer-Büttiker scattering theory in Sec. III, and their reduced expressions in both high temperature and high voltage regimes in Sec. IV. In Secs. V and VI, we apply our results to a QPC and a QD and discuss various regimes. We conclude in Sec. VII.

II. DEFINITIONS

We define the following zero-frequency current correlators between the reservoirs p and q :

$$\mathcal{S}_{pq}^{\alpha\beta} = \int \langle \delta \hat{I}_p^\alpha(t) \delta \hat{I}_q^\beta(0) \rangle dt, \quad (1)$$

where $\delta \hat{I}_p^\alpha(t) = \hat{I}_p^\alpha(t) - I_p^\alpha$, with $\hat{I}_p^{e(h)}$ the charge (heat) current operator, and $I_p^{e(h)} = \langle \hat{I}_p^{e(h)} \rangle$ the charge (heat) average current in the reservoir p . \mathcal{S}_{pq}^{ee} corresponds to the charge noise and \mathcal{S}_{pq}^{hh} corresponds to the heat noise, whereas \mathcal{S}_{pq}^{eh} and \mathcal{S}_{pq}^{he} correspond to the correlations between charge and heat currents. We call them *mixed* noises. In the following, we restrict our work to two terminal systems, i.e. $\{p, q\} \in \{L, R\}$, where L (R) refers to the left (right) reservoir. As a general rule, we call *auto*-quantities when calculated for $p = q$, and *cross*-quantities when calculated for $p \neq q$.

Next, we introduce the differential conductances defined as:

$$G_{L,R} = \frac{\partial I_{L,R}^e}{\partial V_{L,R}}, \quad K_{R,L} = -\frac{\partial I_{L,R}^h}{\partial T_{R,L}}, \quad (2)$$

$$X_{L,R} = \frac{\partial I_{L,R}^e}{\partial T_{L,R}}, \quad Y_{R,L} = -\frac{\partial I_{L,R}^h}{\partial V_{R,L}}. \quad (3)$$

$G_{L,R}$ and $K_{R,L}$ correspond to the electrical and thermal differential conductances, whereas $X_{L,R}$ and $Y_{L,R}$ are “new” differential (mixed) conductances that locally reflect the thermoelectric conversion. In the linear response regime, these two last conductances are related to Seebeck and Peltier coefficients (see Sec. IV A). We will also use average conductances merely defined as: $G = (G_L + G_R)/2$, $X = (X_L + X_R)/2$, $Y = (Y_L + Y_R)/2$, and $K = (K_L + K_R)/2$.

Moreover, we introduce a dimensionless quantity: the ratio between the product of mixed correlations on the one hand, and the product of charge and heat ones on the other hand:

$$r_{pq} = \frac{\mathcal{S}_{pq}^{eh} \mathcal{S}_{pq}^{he}}{\mathcal{S}_{pq}^{ee} \mathcal{S}_{pq}^{hh}}. \quad (4)$$

Whereas $|r_{pp}| \leq 1$ because of the Cauchy-Schwarz inequality, we will show here that no such limitation applies for $r_{p \neq q}$. Notice that in Ref. 33, another type of coefficient was defined for a three-terminal quantum dot engine that could be written $r = [\mathcal{S}_{13}^{eh}]^2 / (\mathcal{S}_{11}^{ee} \mathcal{S}_{33}^{hh})$, it is still bound by the Cauchy-Schwarz inequality $|r| \leq 1$.

III. LANDAUER-LIKE EXPRESSIONS

We derive the formal expressions of the differential conductances, and heat, charge and mixed noises at zero frequency within the Landauer-Büttiker scattering theory.³⁴ We assume that the transmission coefficient \mathcal{T} through the nanoscopic conductor does not depend on the external variables $V_{L,R}$ and $T_{L,R}$.

A. Differential conductances

To get the differential conductances, we use the Landauer expressions of charge and heat average currents:

$$I_{L,R}^e = \pm \frac{e}{h} \int_{-\infty}^{\infty} [f_L(\epsilon) - f_R(\epsilon)] \mathcal{T}(\epsilon) d\epsilon, \quad (5)$$

$$I_{L,R}^h = \pm \frac{1}{h} \int_{-\infty}^{\infty} (\epsilon - eV_{L,R}) [f_L(\epsilon) - f_R(\epsilon)] \mathcal{T}(\epsilon) d\epsilon, \quad (6)$$

where $f_p(\epsilon) = [1 + e^{(\epsilon - eV_p)/(k_B T_p)}]^{-1}$ is the Fermi-Dirac distribution function and the sign $+$ ($-$) holds for reservoir L (R). The convention chosen for the current directions is to consider the flux of electron or heat from the reservoirs to the central part of the system. The calculation of their derivatives according to $V_{L,R}$ or $T_{L,R}$ leads to:

$$G_{L,R} = \frac{e^2}{hk_B T_{L,R}} \int_{-\infty}^{\infty} f_{L,R}(\epsilon) [1 - f_{L,R}(\epsilon)] \mathcal{T}(\epsilon) d\epsilon, \quad (7)$$

$$X_{L,R} = \frac{e}{hk_B T_{L,R}^2} \int_{-\infty}^{\infty} (\epsilon - eV_{L,R}) \times f_{L,R}(\epsilon) [1 - f_{L,R}(\epsilon)] \mathcal{T}(\epsilon) d\epsilon, \quad (8)$$

$$Y_{R,L} = \frac{e}{hk_B T_{R,L}} \int_{-\infty}^{\infty} (\epsilon - eV_{L,R}) \times f_{R,L}(\epsilon) [1 - f_{R,L}(\epsilon)] \mathcal{T}(\epsilon) d\epsilon, \quad (9)$$

and,

$$K_{R,L} = \frac{1}{hk_B T_{R,L}^2} \int_{-\infty}^{\infty} (\epsilon - eV_L)(\epsilon - eV_R) \times f_{R,L}(\epsilon) [1 - f_{R,L}(\epsilon)] \mathcal{T}(\epsilon) d\epsilon. \quad (10)$$

These conductances obey the relation $Y_{R,L} = T_{R,L} X_{R,L} \pm (V_L - V_R) G_{R,L}$ which reduces to $Y_{R,L} = T_{R,L} X_{R,L}$ in the linear response regime (Onsager relation).

B. Current noises

Within the Landauer-Büttiker scattering theory, the zero-frequency charge, charge-heat and heat currents noises are given by:

$$\mathcal{S}_{pq}^{ee} = (2\delta_{pq} - 1) \frac{e^2}{h} \int_{-\infty}^{\infty} \mathcal{F}(\epsilon) d\epsilon, \quad (11)$$

$$\mathcal{S}_{pq}^{eh} = (2\delta_{pq} - 1) \frac{e}{h} \int_{-\infty}^{\infty} (\epsilon - eV_q) \mathcal{F}(\epsilon) d\epsilon, \quad (12)$$

$$\mathcal{S}_{pq}^{he} = (2\delta_{pq} - 1) \frac{e}{h} \int_{-\infty}^{\infty} (\epsilon - eV_p) \mathcal{F}(\epsilon) d\epsilon, \quad (13)$$

and,

$$\mathcal{S}_{pq}^{hh} = (2\delta_{pq} - 1) \frac{1}{h} \int_{-\infty}^{\infty} (\epsilon - eV_p)(\epsilon - eV_q) \mathcal{F}(\epsilon) d\epsilon, \quad (14)$$

where the factor $(2\delta_{pq} - 1)$ gives 1 when $p = q$ and -1 when $p \neq q$, and

$$\begin{aligned} \mathcal{F}(\epsilon) = & \mathcal{T}(\epsilon) [f_L(\epsilon)[1 - f_L(\epsilon)] + f_R(\epsilon)[1 - f_R(\epsilon)] \\ & + \mathcal{T}(\epsilon)[1 - \mathcal{T}(\epsilon)][f_L(\epsilon) - f_R(\epsilon)]^2. \end{aligned} \quad (15)$$

These correlators are related each other. For the charge noises, we have:

$$\mathcal{S}_{pq}^{ee} = \mathcal{S}_{qp}^{ee}, \quad \mathcal{S}_{pp}^{ee} = \mathcal{S}_{\bar{p}\bar{p}}^{ee}, \quad \mathcal{S}_{p\bar{p}}^{ee} = -\mathcal{S}_{\bar{p}p}^{ee}, \quad (16)$$

where $\bar{p} = L$ when $p = R$, and $\bar{p} = R$ when $p = L$. For the mixed noises, we have:

$$\mathcal{S}_{pq}^{eh} = \mathcal{S}_{qp}^{he}, \quad (17)$$

$$\mathcal{S}_{pq}^{eh} = \mathcal{S}_{pq}^{he} + (V_p - V_q) \mathcal{S}_{pq}^{ee}, \quad (18)$$

$$\mathcal{S}_{pp}^{eh} = \mathcal{S}_{\bar{p}\bar{p}}^{eh} + (V_{\bar{p}} - V_p) \mathcal{S}_{pp}^{ee}, \quad (19)$$

$$\mathcal{S}_{p\bar{p}}^{eh} = -\mathcal{S}_{\bar{p}p}^{eh} + (V_{\bar{p}} - V_p) \mathcal{S}_{pp}^{ee}, \quad (20)$$

which reduce to $\mathcal{S}_{pq}^{eh} = \mathcal{S}_{pq}^{he} = \mathcal{S}_{qp}^{he}$, $\mathcal{S}_{pp}^{eh} = \mathcal{S}_{\bar{p}\bar{p}}^{eh}$ and $\mathcal{S}_{p\bar{p}}^{eh} = -\mathcal{S}_{\bar{p}p}^{eh}$ in the linear response regime. For the heat noises, we have:

$$\mathcal{S}_{pq}^{hh} = \mathcal{S}_{qp}^{hh}, \quad (21)$$

$$\mathcal{S}_{pp}^{hh} = \mathcal{S}_{\bar{p}\bar{p}}^{hh} + 2(V_{\bar{p}} - V_p) \mathcal{S}_{\bar{p}\bar{p}}^{eh} + (V_{\bar{p}} - V_p)^2 \mathcal{S}_{\bar{p}\bar{p}}^{ee}, \quad (22)$$

which reduces to $\mathcal{S}_{pp}^{hh} = \mathcal{S}_{\bar{p}\bar{p}}^{hh}$ in the linear response regime. In addition, we deduce:

$$2\mathcal{S}_{p\bar{p}}^{hh} + \mathcal{S}_{pp}^{hh} + \mathcal{S}_{\bar{p}\bar{p}}^{hh} = (V_p - V_{\bar{p}})^2 \mathcal{S}_{pp}^{ee}. \quad (23)$$

As a major consequence of these relations, we conclude that the cross noises and the cross-ratio defined by Eq. (4) in between the two reservoirs is symmetric when we interchange the reservoirs: $\mathcal{S}_{RL}^{\alpha\beta} = \mathcal{S}_{LR}^{\beta\alpha}$ and $r_{RL} = r_{LR}$, thus we will not discuss $\mathcal{S}_{RL}^{\alpha\beta}$ nor r_{RL} in the paper. Inversely, r_{LL} and r_{RR} can be different as we will obtain in the QD nanosystem (see Sec. VI).

C. Relations between noises and differential conductances

We want to express noises in terms of differential conductance defined in Sec. II. Reporting Eqs. (7), (8), (9) and (10) in the expressions of the charge, mixed and heat correlators given by Eqs. (11), (12), (13), and (14), we get:

$$\mathcal{S}_{pq}^{ee} = (2\delta_{pq} - 1) [k_B T_L G_L + k_B T_R G_R] + (2\delta_{pq} - 1) \frac{e^2}{h} \int_{-\infty}^{\infty} \mathcal{T}(\epsilon) [1 - \mathcal{T}(\epsilon)] [f_L(\epsilon) - f_R(\epsilon)]^2 d\epsilon, \quad (24)$$

$$\mathcal{S}_{pq}^{eh} = (2\delta_{pq} - 1) [k_B T_q^2 X_q + k_B T_{\bar{q}}^2 Y_{\bar{q}}] + (2\delta_{pq} - 1) \frac{e}{h} \int_{-\infty}^{\infty} (\epsilon - eV_q) \mathcal{T}(\epsilon) [1 - \mathcal{T}(\epsilon)] [f_L(\epsilon) - f_R(\epsilon)]^2 d\epsilon, \quad (25)$$

$$\mathcal{S}_{pq}^{he} = (2\delta_{pq} - 1) [k_B T_p^2 X_p + k_B T_{\bar{p}}^2 Y_{\bar{p}}] + (2\delta_{pq} - 1) \frac{e}{h} \int_{-\infty}^{\infty} (\epsilon - eV_p) \mathcal{T}(\epsilon) [1 - \mathcal{T}(\epsilon)] [f_L(\epsilon) - f_R(\epsilon)]^2 d\epsilon, \quad (26)$$

$$\begin{aligned} \mathcal{S}_{pq}^{hh} = & (2\delta_{pq} - 1) [k_B T_L^2 K_L + k_B T_R^2 K_R] + \delta_{pq} (V_{\bar{p}} - V_p) [k_B T_p^2 X_p + k_B T_{\bar{p}}^2 Y_{\bar{p}}] / e \\ & + (2\delta_{pq} - 1) \frac{1}{h} \int_{-\infty}^{\infty} (\epsilon - eV_p)(\epsilon - eV_q) \mathcal{T}(\epsilon) [1 - \mathcal{T}(\epsilon)] [f_L(\epsilon) - f_R(\epsilon)]^2 d\epsilon. \end{aligned} \quad (27)$$

With the help of these relations, we can discuss in a quite direct way the behaviors of noises in various regimes as done in the next section.

IV. HIGH TEMPERATURE AND HIGH VOLTAGE REGIMES

From now, we specify $V_{L,R}$ and $T_{L,R}$ in terms of voltage gradient V and temperature gradient T between the reservoirs: $V_{L,R} = \pm V/2$ and $T_{L,R} = T_0 \pm T/2$, where T_0 is the average temperature of the system.

A. High temperature regime ($k_B T_0 \gg eV$)

In that regime, the last contributions in Eqs. (24), (25), (26) and (27) are negligible, thus we can write these formula in terms of differential conductances. We find:

$$\mathcal{S}_{LL}^{ee} = \mathcal{S}_{RR}^{ee} = k_B T_L G_L + k_B T_R G_R = -\mathcal{S}_{LR}^{ee}, \quad (28)$$

$$\mathcal{S}_{LL}^{eh} = \mathcal{S}_{LL}^{he} = k_B T_L^2 X_L + k_B T_R Y_R = -\mathcal{S}_{LR}^{he}, \quad (29)$$

$$\mathcal{S}_{RR}^{eh} = \mathcal{S}_{RR}^{he} = k_B T_R^2 X_R + k_B T_L Y_L = -\mathcal{S}_{LR}^{eh}, \quad (30)$$

$$\mathcal{S}_{LL}^{hh} = \mathcal{S}_{RR}^{hh} = k_B T_L^2 K_L + k_B T_R^2 K_R = -\mathcal{S}_{LR}^{hh}. \quad (31)$$

We remark that auto- and cross-correlations have the same absolute value. In addition, from Eqs. (12) and (13), it can be shown that $\mathcal{S}_{LL}^{eh} = \mathcal{S}_{RR}^{eh}$ which leads to $T_L^2 X_L + T_R Y_R = T_R^2 X_R + T_L Y_L$, in full agreement with the Onsager relation $Y_{L,R} = T_{L,R} X_{L,R}$. For equal left and right temperatures, i.e. T goes to zero, we are back to the linear response regime which gives $Y = X T_0$ as already mentioned in Sec. III.A., and the noises simplify to:

$$\mathcal{S}_{LL}^{ee} = \mathcal{S}_{RR}^{ee} = 2k_B T_0 G = -\mathcal{S}_{LR}^{ee}, \quad (32)$$

$$\mathcal{S}_{LL}^{eh} = \mathcal{S}_{RR}^{eh} = 2k_B T_0^2 X = -\mathcal{S}_{LR}^{he}, \quad (33)$$

$$\mathcal{S}_{LL}^{he} = \mathcal{S}_{RR}^{he} = 2k_B T_0 Y = -\mathcal{S}_{LR}^{eh}, \quad (34)$$

$$\mathcal{S}_{LL}^{hh} = \mathcal{S}_{RR}^{hh} = 2k_B T_0^2 K = -\mathcal{S}_{LR}^{hh}. \quad (35)$$

Equations (32) and (35) correspond to the fluctuation-dissipation theorems for the charge and heat noises respectively. We find here that it exists also direct links

between mixed noises and thermoelectric conductances X and Y given by Eqs. (33) and (34), in agreement with Ref. 33.

From Eqs. (32), (33), (34) and (35), we directly deduced that all auto- and cross-ratios are identical in the linear limit:

$$r_{LL} = r_{RR} = r_{LR}. \quad (36)$$

In addition, it can be shown that X and Y are related to the Seebeck S and Peltier Π coefficients through the relations:

$$X = -GS, \quad (37)$$

$$Y = -\Pi G = -S T_0 G. \quad (38)$$

With the help of these results, the thermoelectric figure of merit, defined as $ZT_0 = S^2 T_0 G / K$, can be fully expressed either in terms of differential conductances, or in terms of the noises defined in Sec. II. Indeed, from Eqs. (32) to (38), we get:

$$ZT_0 = \frac{XY}{GK} = \frac{S_{pq}^{eh} S_{pq}^{he}}{S_{pq}^{ee} S_{pq}^{hh}} = r_{pq}, \quad (39)$$

which is verified whatever is the choice of the reservoirs p and q . Thus, in the linear response regime, the figure of merit for thermoelectricity is given by the ratio between the product of mixed noises and the product of heat and charge noises. This ratio is hence relevant to quantify the efficiency of thermoelectric conversion. Because of the Cauchy-Swartz inequality, we have $S_{pp}^{eh} S_{pp}^{he} < S_{pp}^{ee} S_{pp}^{hh}$. As a major consequence, the maximal value that ZT_0 can taken in the linear regime is 1 in agreement with Ref. 35. Thus, all experiments with a measured ZT_0 above one operate in the non-linear regime for which the use of the figure of merit to quantify the efficiency is questionable.

B. High voltage regime ($eV \gg k_B T_0$)

In that regime, the first and second contributions in Eqs. (24), (25), (26) and (27) are negligible and we set $T_{L,R}$ to zero, thus:

$$\mathcal{S}_{LL}^{ee} = \frac{e^2}{h} \text{sign}(V) \int_{-eV/2}^{eV/2} \mathcal{T}(\epsilon) [1 - \mathcal{T}(\epsilon)] d\epsilon = -\mathcal{S}_{LR}^{ee}, \quad (40)$$

$$\mathcal{S}_{LL}^{eh} = \frac{e}{h} \text{sign}(V) \int_{-eV/2}^{eV/2} \left(\epsilon - \frac{eV}{2} \right) \mathcal{T}(\epsilon) [1 - \mathcal{T}(\epsilon)] d\epsilon = -\mathcal{S}_{LR}^{he}, \quad (41)$$

$$\mathcal{S}_{RR}^{he} = \frac{e}{h} \text{sign}(V) \int_{-eV/2}^{eV/2} \left(\epsilon + \frac{eV}{2} \right) \mathcal{T}(\epsilon) [1 - \mathcal{T}(\epsilon)] d\epsilon = -\mathcal{S}_{LR}^{eh}, \quad (42)$$

$$\mathcal{S}_{LL}^{hh} = \frac{1}{h} \text{sign}(V) \int_{-eV/2}^{eV/2} \left(\epsilon - \frac{eV}{2} \right)^2 \mathcal{T}(\epsilon) [1 - \mathcal{T}(\epsilon)] d\epsilon, \quad (43)$$

$$\mathcal{S}_{RR}^{hh} = \frac{1}{h} \text{sign}(V) \int_{-eV/2}^{eV/2} \left(\epsilon + \frac{eV}{2} \right)^2 \mathcal{T}(\epsilon) [1 - \mathcal{T}(\epsilon)] d\epsilon, \quad (44)$$

$$\mathcal{S}_{LR}^{hh} = -\frac{1}{h} \text{sign}(V) \int_{-eV/2}^{eV/2} \left(\epsilon^2 - \frac{e^2 V^2}{4} \right) \mathcal{T}(\epsilon) [1 - \mathcal{T}(\epsilon)] d\epsilon. \quad (45)$$

Contrary to what happens in the high temperature regime, the heat auto- and cross-correlators take here distinct values.

We now focus on two concrete nanosystems namely a quantum point contact and a quantum dot to further examine these correlators and the ratios of noises we have introduced.

V. APPLICATION TO A QUANTUM POINT CONTACT

The first application of our results concerns a quantum point contact in an ohmic environment whose resistance is equal to $R_Q = h/e^2$ (see Fig. 1). Because of this coupling with environment, measured by Γ , its transmission coefficient acquires an energy dependency: $\mathcal{T}(\epsilon) = \epsilon^2/(\epsilon^2 + \Gamma^2)$. This energy dependency is obtained by the means of a mapping between this system and a Luttinger liquid with a single impurity and interactions parameter equal to one half^{36–39} allowing us to perform a refermionization procedure.^{40,41} Since this system exhibits an electron-hole symmetry, the thermoelectric differential conductances X and Y are equal to zero. We will show that it is also the case for the mixed noises \mathcal{S}_{pq}^{eh} and \mathcal{S}_{pq}^{he} in the high temperature regime but not in the high voltage regime.

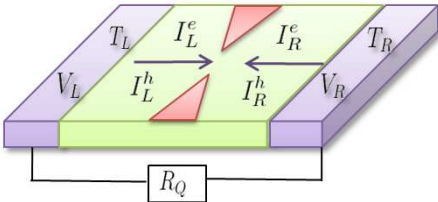


FIG. 1: Picture of the QPC coupled with an ohmic environment, and conventions chosen for left/right currents.

A. High temperature regime ($k_B T_0 \gg eV$)

We first focus on the case where the temperatures of the reservoirs are identical, $T_{L,R} = T_0$, and large in comparison to the applied voltage. Since X and Y are equal to zero, but not G and K (see Tab. I), the resulting figure of merit, such as the ratio of noises, cancels because of Eq. (39). From Eqs. (32), (33), (34) and (35), we deduce the noises and give their equivalent expressions in Tab. I. When the temperature is the largest energy scale of the problem, the electrical and thermal conductances take constant values: G_Q and K_Q , where $G_Q = e^2/h$ is the quantum of electrical conductance, and $K_Q = \pi^2 k_B^2 T_0 / 3h$ is the quantum of thermal conductance recently measured in such a system.⁴²

QPC	$\{eV, \Gamma\} \ll k_B T_0$	$eV \ll k_B T_0 \ll \Gamma$
G	G_Q	$\frac{\pi^2}{3} \left(\frac{k_B T_0}{\Gamma} \right)^2 G_Q$
X, Y	0	0
K	K_Q	$\frac{7\pi^2}{5} \left(\frac{k_B T_0}{\Gamma} \right)^2 K_Q$
$\mathcal{S}_{LL}^{ee} = -\mathcal{S}_{LR}^{ee} = 2k_B T_0 G$	$2k_B T_0 G_Q$	$\frac{2\pi^2}{3} \frac{(k_B T_0)^3}{\Gamma^2} G_Q$
$\mathcal{S}_{LL}^{eh} = -\mathcal{S}_{LR}^{eh} = 2k_B T_0 Y$	0	0
$\mathcal{S}_{LL}^{hh} = -\mathcal{S}_{LR}^{hh} = 2k_B T_0^2 K$	$2k_B T_0^2 K_Q$	$\frac{14\pi^2}{5} \frac{k_B^3 T_0^4}{\Gamma^2} K_Q$
$r_{LL} = r_{RR} = r_{LR}$	0	0

TABLE I: High temperature regime in a QPC – Equivalent expressions of the differential conductances, noises and ratios of noises obtained for $V = 0$ and $T_{L,R} = T_0$.

Figure 2 shows the crossover between the temperature power laws of the differential conductances G and K at strong coupling Γ with the environment and their constant limits G_Q and K_Q at weak Γ which corresponds to a QPC decoupled from the ohmic environment. Notice that the Wiedemann-Franz relation between electrical and thermal conductances does not apply except when the temperature is the largest energy scale (see the

central column of Tab. I). In that case:

$$\frac{K}{GT_0} = \frac{K_Q}{G_Q T_0} = \frac{\pi^2 k_B^2}{3e^2} = \mathcal{L}, \quad (46)$$

which is the Lorenz factor. Identically, $\mathcal{S}_{pq}^{hh}/(\mathcal{S}_{pq}^{ee} T_0) = \mathcal{L}$ in that regime.

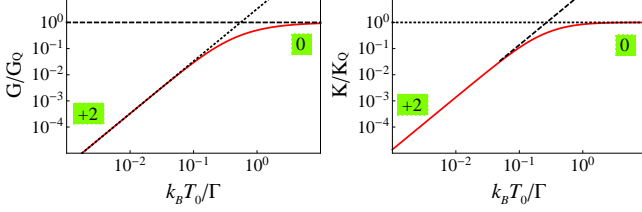


FIG. 2: High temperature regime in a QPC – Differential conductances G and K as a function of the average temperature T_0 for $V = 0$ and $T = 0$. X and Y are not shown since they are equal to zero in that regime. As a consequence, the associated ratios r_{pq} cancel. The exponents of the power laws obtained in the equivalent expressions Tab. I are indicated in the green squares, and their signatures are represented by dashed lines.

B. High voltage regime ($eV \gg k_B T_0$)

We turn now our interest to the case where the applied voltage is large in comparison to the temperature. In that limit, the integrals of Eqs. (40), (41), (42), (43), (44) and (45) can be performed analytically (see Appendix A for the expressions of the currents and noises). The equivalent expressions of the differential conductances, noises and ratios of noises are given in Tab. II. Only the electrical conductance is relevant in this regime since $X = Y = K = 0$. We see that G does not depend on voltage when eV is the largest energy of the problem (central column of Tab. II).

Due to the parity of the QPC transmission \mathcal{T} , the heat auto-correlators do not depend on the reservoir: $\mathcal{S}_{LL}^{hh} = \mathcal{S}_{RR}^{hh}$. This property ensures identical auto-ratios $r_{LL} = r_{RR}$. Comparing the central and the last columns of Tab. II, we remark that $\mathcal{S}_{LL}^{eh} = -(V/2)\mathcal{S}_{LL}^{ee}$ and $\mathcal{S}_{LL}^{hh} \propto -(V/2)\mathcal{S}_{LL}^{eh}$ (idem for the cross-noises). The proportionality coefficient is exactly 1 when $\{k_B T_0, \Gamma\} \ll eV$, while for $k_B T_0 \ll eV \ll \Gamma$, it is above one ($8/5$) for the auto-noises and below one ($2/5$) for the cross-noises, which gives $r_{LL} < 1$ and $r_{LR} > 1$ respectively (see the central and the last columns of Tab. IV).

The left graph of Fig. 3 shows the variation of the electrical conductance as a function of the voltage. By comparing the last columns of Tabs. I and II, we notice that the power law exponent obtained in the limit $k_B T_0 \ll eV \ll \Gamma$, for which $G \propto (eV/\Gamma)^2$, is the same than the one obtained in the limit $eV \ll k_B T_0 \ll \Gamma$ for which $G \propto (k_B T_0/\Gamma)^2$, meaning that temperature and voltage

QPC	$\{k_B T_0, \Gamma\} \ll eV$	$k_B T_0 \ll eV \ll \Gamma$
G	G_Q	$(\frac{eV}{2\Gamma})^2 G_Q$
X, Y, K	0	0
$\mathcal{S}_{LL}^{ee} = -\mathcal{S}_{LR}^{ee}$	$\frac{\pi\Gamma}{2} G_Q$	$\frac{e^3 V ^3}{12\Gamma^2} G_Q = \frac{e V }{3} G$
$\mathcal{S}_{LL}^{eh} = -\mathcal{S}_{RR}^{eh} = -\mathcal{S}_{LR}^{he}$	$-\frac{\pi\Gamma V}{4} G_Q = -\frac{V}{2} \mathcal{S}_{LL}^{ee}$	$-\frac{e^3 V ^3 V}{24\Gamma^2} G_Q = -\frac{V}{2} \mathcal{S}_{LL}^{ee}$
$\mathcal{S}_{LL}^{hh} = \mathcal{S}_{RR}^{hh}$	$\frac{\pi\Gamma V^2}{8} G_Q = \frac{V^2}{4} \mathcal{S}_{LL}^{ee}$	$\frac{e^3 V ^5}{30\Gamma^2} G_Q = \frac{2V^2}{5} \mathcal{S}_{LL}^{ee}$
\mathcal{S}_{LR}^{hh}	$\frac{\pi\Gamma V^2}{8} G_Q = -\frac{V^2}{4} \mathcal{S}_{LR}^{ee}$	$\frac{e^3 V ^5}{120\Gamma^2} G_Q = -\frac{V^2}{10} \mathcal{S}_{LR}^{ee}$
$r_{LL} = r_{RR}$	1	5/8
r_{LR}	1	5/2

TABLE II: High voltage regime in a QPC – Equivalent expressions of the differential conductances, noises and ratios of noises obtained for $T_{L,R} = 0$.

play a similar role for the electrical conductance.⁴³ It is not the case for the thermal conductance that vanishes in the high voltage regime, whereas it follows a power law in the high temperature regime.

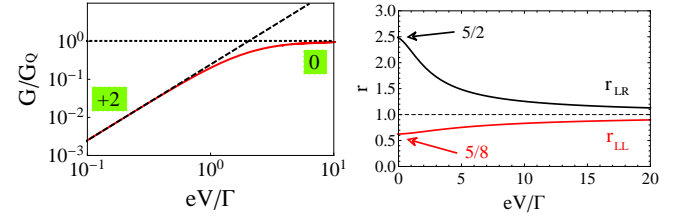


FIG. 3: High voltage regime in a QPC – Left: differential conductance G (red line), power law exponents (in green squares) and signatures (dashed lines) of their equivalent expressions given Tab. II. Right: noises ratios ($r_{LL} = r_{RR}$) as a function of the voltage at zero temperatures.

Contrary to what happens in the high temperature regime, the ratios of noises are non-zero in the high voltage regime. Interestingly, whereas r_{LL} stays below one when varying voltage, the cross-ratio r_{LR} exhibits a value larger than one (up to $5/2$) in the strong coupling limit as shown in the right graph of Fig. 3, where the equivalent expressions given in Tab. II are recovered in both $eV/\Gamma \ll 1$ and $eV/\Gamma \gg 1$ limits.

VI. APPLICATION TO A QUANTUM DOT

We now consider a single level non-interacting quantum dot with a transmission coefficient $\mathcal{T}(\epsilon) = \Gamma^2/[(\epsilon - \epsilon_0)^2 + \Gamma^2]$, where ϵ_0 is the energy level of the dot (see Fig. 4), and Γ is the broadening due to the contact to the reservoirs which is assumed to be energy independent and symmetrical $\Gamma_L = \Gamma_R = \Gamma$.

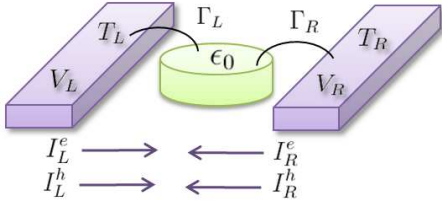


FIG. 4: Picture of the QD and conventions chosen for left/right currents.

A. High temperature regime ($k_B T_0 \gg eV$)

In Fig. 5 are plotted differential conductances as well as their equivalent expressions summarized in Table III. For both limits $k_B T_0 \ll \Gamma$ and $k_B T_0 \gg \Gamma$, these quantities exhibit power laws with various exponents. Notice that X , Y , S_{pq}^{eh} , S_{pq}^{he} and r_{pq} all cancel when electron-hole symmetry applied, i.e. $\epsilon_0 = 0$, and thus we recover for the noises the results obtained in the QPC since in that case $\mathcal{T}_{\text{QD}}(\epsilon) = 1 - \mathcal{T}_{\text{QPC}}(\epsilon)$ (compare the central column of Tab. I and the last column of Tab. III).

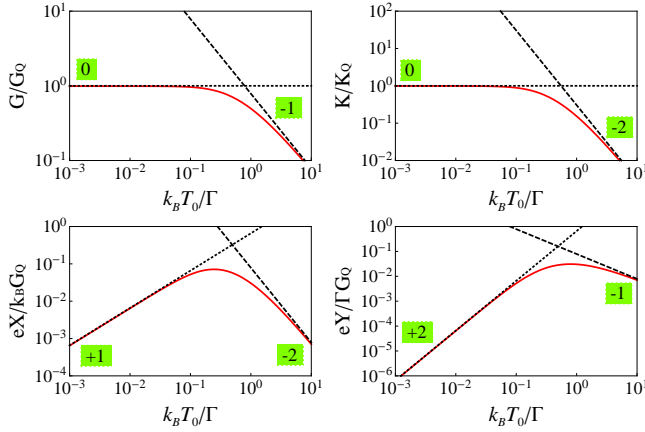


FIG. 5: High temperature regime in a QD – Differential conductances as a function of the average temperature for $V = 0$, $T = 0$, and $\epsilon_0/\Gamma = 0.1$. Power law exponents (in green squares) and signatures (dashed lines) of their equivalent expressions given Tab. III.

From Tab. III, we also see that the differential conductances X and Y are proportional to the dot energy level in agreement with the fact that thermoelectric measurements in the high temperature regime give indication on the position of the dot energy level relatively to the Fermi energy.⁴⁴ We find here that because of the fluctuation-dissipation theorem, the mixed noises are themselves proportional to the dot energy level.

In addition, the ratios r_{LL} and r_{LR} are equal to each other and they correspond to XY/GK since the fluctuation-dissipation theorem applies. Figure 6 shows the evolution of these ratios as a function of T_0 and ϵ_0 in

QD	$\{eV, \Gamma\} \ll k_B T_0$	$eV \ll k_B T_0 \ll \Gamma$
G	$\frac{\pi}{4} \left(\frac{\Gamma}{k_B T_0} \right) G_Q$	G_Q
$Y = XT_0$	$\frac{\pi \epsilon_0}{4e} \left(\frac{\Gamma}{k_B T_0} \right) G_Q$	$\frac{2\pi^2 \epsilon_0}{3e} \left(\frac{k_B T_0}{\Gamma} \right)^2 G_Q$
K	$\frac{3}{\pi^2} \left(\frac{\Gamma}{k_B T_0} \right)^2 K_Q$	K_Q
$S_{LL}^{ee} = -S_{LR}^{ee} = 2k_B T_0 G$	$\frac{\pi \Gamma}{2} G_Q$	$2k_B T_0 G_Q$
$S_{LL}^{eh} = -S_{LR}^{eh} = 2k_B T_0 Y$	$\frac{\pi \Gamma \epsilon_0}{2e} G_Q$	$\frac{4\pi^2}{3e} \left(\frac{k_B T_0}{\Gamma} \right)^3 \Gamma \epsilon_0 G_Q$
$S_{LL}^{hh} = -S_{LR}^{hh} = 2k_B T_0^2 K$	$\frac{6\Gamma^2}{\pi^2 k_B} K_Q$	$2k_B T_0^2 K_Q$
$r_{LL} = r_{RR} = r_{LR}$	$\frac{\pi}{4} \frac{\epsilon_0^2}{\Gamma k_B T_0} = \frac{XY}{GK}$	$\frac{4\pi^2}{3} \left(\frac{k_B T_0 \epsilon_0}{\Gamma^2} \right)^2 = \frac{XY}{GK}$

TABLE III: High temperature regime in a QD – Equivalent expressions of the differential conductances, noises and ratios of noises obtained for $V = 0$, $T_{L,R} = T_0$, and $\epsilon_0 \ll \Gamma$.

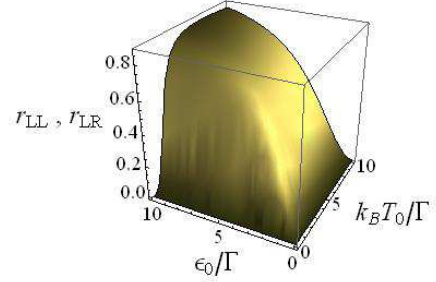


FIG. 6: High temperature regime in a QD – Variation of the ratios $r_{LL} = r_{RR} = r_{LR}$ as a function of temperature T_0 and dot energy level ϵ_0 for equal left and right temperatures at zero voltage.

the absence of any temperature gradient. They vanish at $\epsilon_0 = 0$ as expected and their maximum does not exceed one even for large values of ϵ_0 because of the Cauchy-Schwarz inequality.

B. High voltage regime ($eV \gg k_B T_0$)

In that regime, the differential electrical conductance reads as $G = (G_Q/2) \sum_{\pm} \Gamma^2 / [(\epsilon_0 \pm eV/2)^2 + \Gamma^2]$, and we have: $K = X = Y = 0$. The integrals of Eqs. (40), (41), (42), (43), (44) and (45) are performed analytically (see Appendix B for the expressions of the currents and noises). The equivalent expressions of conductances and noises are given in Tab. IV. Same as in the QPC, we find that heat, charge and mixed noises are strongly related to each other via the voltage, since

we have $\mathcal{S}_{LL}^{eh} = -(V/2)\mathcal{S}_{LL}^{ee}$ and $\mathcal{S}_{LR}^{he} = -(V/2)\mathcal{S}_{LR}^{ee}$ in all cases, and moreover $\mathcal{S}_{LL}^{hh} \propto -(V/2)\mathcal{S}_{LL}^{eh} \propto (V^2/4)\mathcal{S}_{LL}^{ee}$ and $\mathcal{S}_{LR}^{hh} \propto (V/2)\mathcal{S}_{LR}^{he} \propto -(V^2/4)\mathcal{S}_{LR}^{ee}$. For a strict equality, both auto- and cross-ratios of noises reach one. Otherwise, the proportionality coefficients give $r_{LL} < 1$ and $r_{LR} > 1$ and stay unchanged as long as eV stays the lowest energy of the problem excluding temperature (com-

pare the second and third columns of Tab. IV).

In Tab. IV, the expressions for \mathcal{S}_{LL}^{hh} and \mathcal{S}_{RR}^{hh} , and hence for auto-ratios, are identical in the three limits we consider. This is no longer the case in intermediate regimes, in contrast with the QPC, as shown Figs. 7 and 8. Indeed, $\mathcal{T}_{QD}(\epsilon)$ is no longer even when $\epsilon_0 \neq 0$ which results in $\mathcal{S}_{LL}^{hh} \neq \mathcal{S}_{RR}^{hh}$.

QD	$\{eV, \Gamma\} \ll \epsilon_0$	$\{eV, \epsilon_0\} \ll \Gamma$	$\{\Gamma, \epsilon_0\} \ll eV$
G	$\frac{\Gamma^2}{\epsilon_0^2} G_Q$	G_Q	$\frac{4\Gamma^2}{\epsilon^2 V^2} G_Q$
X, Y, K	0	0	0
$\mathcal{S}_{LL}^{ee} = -\mathcal{S}_{LR}^{ee}$	$(\frac{\Gamma}{\epsilon_0})^2 e V G_Q = e V G$	$(\frac{\epsilon_0}{\Gamma})^2 e V G_Q$	$\frac{\pi\Gamma}{2} G_Q = \frac{\pi e^2 V^2}{2\Gamma} G$
$\mathcal{S}_{LL}^{eh} = -\mathcal{S}_{LR}^{he}$	$-(\frac{\Gamma}{\epsilon_0})^2 \frac{e V }{2} G_Q = -\frac{V}{2} \mathcal{S}_{LL}^{ee}$	$-(\frac{\epsilon_0}{\Gamma})^2 \frac{e V }{2} G_Q = -\frac{V}{2} \mathcal{S}_{LL}^{ee}$	$-\frac{\pi\Gamma V}{4} G_Q = -\frac{V}{2} \mathcal{S}_{LL}^{ee}$
$\mathcal{S}_{LL}^{hh} = \mathcal{S}_{RR}^{hh}$	$(\frac{\Gamma}{\epsilon_0})^2 \frac{e V ^3}{3} G_Q = \frac{V^2}{3} \mathcal{S}_{LL}^{ee}$	$(\frac{\epsilon_0}{\Gamma})^2 \frac{e V ^3}{3} G_Q = \frac{V^2}{3} \mathcal{S}_{LL}^{ee}$	$\frac{\pi\Gamma V^2}{8} G_Q = \frac{V^2}{4} \mathcal{S}_{LL}^{ee}$
\mathcal{S}_{LR}^{hh}	$(\frac{\Gamma}{\epsilon_0})^2 \frac{e V ^3}{6} G_Q = -\frac{V^2}{6} \mathcal{S}_{LR}^{ee}$	$(\frac{\epsilon_0}{\Gamma})^2 \frac{e V ^3}{6} G_Q = -\frac{V^2}{6} \mathcal{S}_{LR}^{ee}$	$\frac{\pi\Gamma V^2}{8} G_Q = -\frac{V^2}{4} \mathcal{S}_{LR}^{ee}$
$r_{LL} = r_{RR}$	3/4	3/4	1
r_{LR}	3/2	3/2	1

TABLE IV: High voltage regime in a QD – Equivalent expressions of the differential conductances, noises and ratios of noises obtained for $T_{L,R} = 0$. We stress that heat auto-correlators and auto-ratios reach identical expressions only in the limits reported in this table (see Figs. 7 and 8).

Comparing auto- and cross-ratios Fig. 7, we see that they take distinct values in the high voltage regime, inversely to what happens in the high temperature regime, because of the distinct values taken by \mathcal{S}_{LL}^{hh} and \mathcal{S}_{LR}^{hh} . Same as for the QPC, the cross-ratio r_{LR} can have a value larger than one, whereas r_{LL} and r_{RR} stay always smaller than one, in agreement with the Cauchy-Schwarz inequality. At zero voltage and non-zero ϵ_0 , we recover the fractional values 3/4 for r_{LL} (r_{RR}), and 3/2 for r_{LR} as expected from Tab. IV. At both zero voltage and dot energy level, we recover the fractional values 5/8 for r_{LL} (r_{RR}), and 5/2 for r_{LR} as expected from Tab. II.

C. Intermediate regime

Finally, we propose to further examine the noise ratios in the intermediate regime. Figure 8 shows these ratios as a function of voltage and temperature gradients without any limitation on their relative values. For this particular QD working, all ratios remain almost insensitive to the temperature gradient while they vary strongly with the voltage. Auto- and cross-ratios are still distinct. Remarkably, r_{LR} exhibits a divergence at a voltage value for which \mathcal{S}_{LR}^{hh} cancels as shown Fig. 9. The sign of the auto-correlators in the right reservoir stays positive whatever the values of voltage and temperature are, whereas the mixed auto-correlators in the left reservoir show a sign inversion which does not affect the product $\mathcal{S}_{LL}^{eh}\mathcal{S}_{LL}^{he}$.

The cross-ratio r_{LR} changes sign twice: once with \mathcal{S}_{LR}^{he} (see Fig. 9), and the other at a larger voltage due to the change of sign of \mathcal{S}_{LR}^{hh} giving the divergence of r_{LR} . Indeed, the heat cross-correlator, which is negative at low voltage, becomes positive at high voltage due to the contribution of the term $(V_L - V_R)^2 \mathcal{S}_{LL}^{ee}$ in its expression (see Eq. (23)). For a QPC working in the same conditions (not shown here), the charge and heat noises in the same reservoirs, \mathcal{S}_{LL}^{ee} and \mathcal{S}_{LL}^{hh} , stay positive whereas the mixed noises, \mathcal{S}_{LL}^{eh} and \mathcal{S}_{LL}^{he} , can take negative values as for the QD. The charge noise between distinct reservoirs, \mathcal{S}_{LR}^{ee} is negative while its heat counterpart \mathcal{S}_{LR}^{hh} is positive in that regime. Thus, for the two nanosystems we have considered here, the results are in agreement with Ref. 31 where it has been shown that the heat cross-correlator \mathcal{S}_{LR}^{hh} is not necessary negative, contrary to the charge cross-correlator \mathcal{S}_{LR}^{ee} .

VII. CONCLUSION

We investigated mixed, charge and heat zero-frequency noises in thermoelectric nanosystems connected to reservoirs using Landauer-Büttiker formalism. In the future perspective of studying thermoelectric conversion, we explored two routes. On the one hand, we developed relations between the noises and thermoelectric differential conductances G , K , X and Y we defined which are the adequate quantities to consider in the non-linear

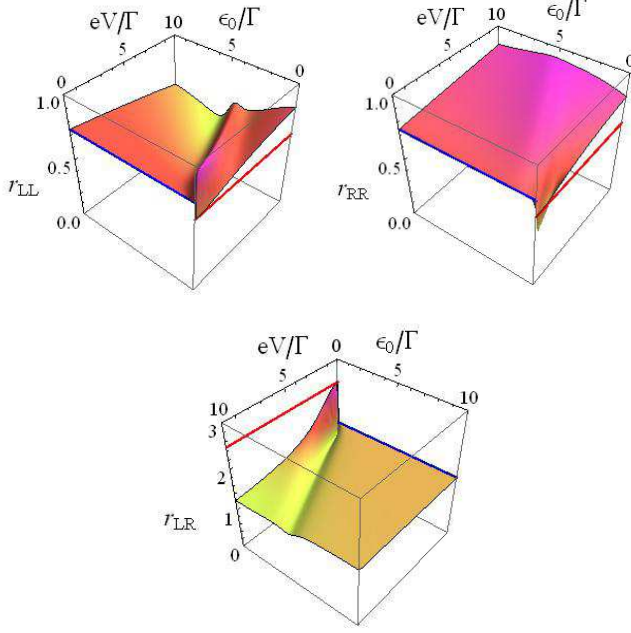


FIG. 7: High voltage regime in a QD – Variation of the ratios r_{LL} , r_{RR} and r_{LR} as a function of voltage and dot energy level at zero temperatures. On both graphs, the red lines indicates their values in the limit $\epsilon_0 = eV = 0$ (i.e., $r_{LL} = r_{RR} = 5/8$ and $r_{LR} = 5/2$) and the blue lines in the limit $eV \ll \epsilon_0$ (i.e., $r_{LL} = r_{RR} = 3/4$ and $r_{LR} = 3/2$).

regime. On the other hand, we interconnected the different noises via ratios of the product of mixed noises divided by the product of charge and heat noises, calculated inside the same reservoir (r_{LL} and r_{RR}) or in between two ($r_{LR} = r_{RL}$). From general derivations, we are able to obtain analytical expressions for differential conductances and noises in various limits. The strategy was thus to exploit them in the linear regime of high temperature, and in the non-linear regime of high voltage in two related nanosystems: a quantum point contact and a quantum dot. Our main conclusions follow.

The mixed conductances X and Y are related to the Seebeck and Peltier coefficients in the linear response regime, and the figure of merit is thus given by $ZT_0 = XY/GK$. Applying our results to a QPC and a QD, we recover the fact that the differential conductances X and Y cancel for systems with electron-hole symmetry. The same applies for the mixed noises \mathcal{S}_{pq}^{eh} and the ratios of noises r_{pq} in the high temperature regime. Inversely in the non-linear high voltage regime, X and Y still cancel for $\epsilon_0 = 0$, but not \mathcal{S}_{pq}^{eh} , nor r_{pq} . It allows us to conclude that the ratio of noises is no longer related to the ratio of differential conductances in the non-linear regime.

The correlations between heat and charge currents provide indication about the efficiency of thermoelectric conversion in the linear response regime. Indeed, we have shown that the figure of merit ZT_0 is given by the square

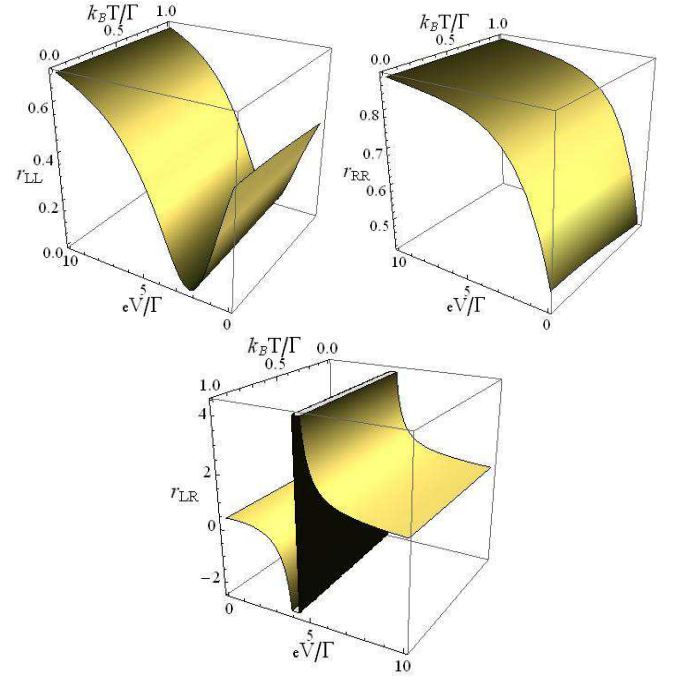


FIG. 8: Intermediate regime in a QD – Variation of the ratios r_{LL} , r_{RR} and r_{LR} as a function of the voltage and the temperature gradients. We take $\epsilon_0/\Gamma = 2$ and $k_B T_0/\Gamma = 1$.

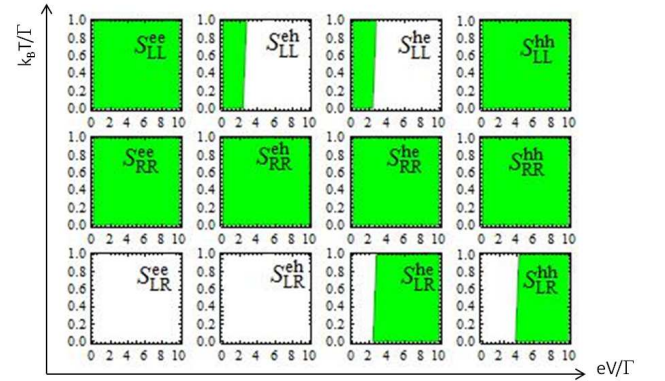


FIG. 9: Intermediate regime in a QD – Regions of positive sign (in green) for auto- and cross-correlators at $\epsilon_0/\Gamma = 2$ and $k_B T_0/\Gamma = 1$. Mixed noises \mathcal{S}_{LL}^{eh} , \mathcal{S}_{LL}^{he} and \mathcal{S}_{LR}^{he} change sign along the same line. The heat cross-noise \mathcal{S}_{LR}^{hh} change sign on an other contour that gives the cross-ratio divergence shown Fig. 8.

of this mixed noise divided by the product of charge noise by heat noise. As a consequence, ZT_0 can not take a value larger than one in that regime. Moreover, choosing auto-correlations (in the same reservoir), or cross-correlations (between distinct reservoirs) leads to the same ratio of noises. This is no longer the case in the high voltage regime, where $r_{LL} = r_{RR}$, but r_{LL} and r_{LR} take different values: because of the Cauchy-Schwarz inequality, r_{LL}

and r_{RR} stay smaller than one whereas there is no limitation for r_{LR} . The situation is more complex in intermediate regime, where the two auto-ratios r_{LL} and r_{RR} are different and show an asymmetry arising from different heat noises in the two reservoirs. Moreover, the cross-ratio exhibits a divergence in the QD that occurs when the heat cross-correlation changes sign varying temperature and voltage gradients.

The cross-ratio r_{LR} , introduced for the first time in this paper, deserves to be studied on an equal footing than r_{LL} and r_{RR} since it measures how the heat current in one reservoir and the charge current in the other are related to each other. Knowing that the figure of merit is no longer connected to thermoelectric efficiency in the non-linear regime,²⁴ it is needed to find a new parameter which informs about the efficiency: these ratios of noises are a possible track to further validate.

Acknowledgments

A.C. thanks Marine Guigou for interesting discussions.

Appendix A: QPC currents and noises in the high voltage regime

Taking $T_L = T_R = 0$, the integrals in the expressions of the currents given by Eqs. (5) and (6) can be performed analytically:

$$I_{L,R}^e = \pm \frac{e}{h} \left[eV - 2\Gamma \arctan\left(\frac{eV}{2\Gamma}\right) \right], \quad (\text{A1})$$

$$I_{L,R}^h = \mp \frac{V}{2} I_{L,R}^e. \quad (\text{A2})$$

The same applies for the expressions of the noises of Eqs. (40), (41), (42), (43), (44) and (45). We obtain for the auto-correlators:

$$\begin{aligned} \mathcal{S}_{LL}^{ee} &= \frac{e^2}{h} \text{sign}(V) \left[-\frac{eV\Gamma^2}{2[\Gamma^2 + (eV/2)^2]} \right. \\ &\quad \left. + \Gamma \arctan\left(\frac{eV}{2\Gamma}\right) \right], \end{aligned} \quad (\text{A3})$$

$$\begin{aligned} \mathcal{S}_{LL}^{eh} &= \frac{e}{h} \text{sign}(V) \left[\frac{(eV\Gamma)^2}{4[\Gamma^2 + (eV/2)^2]} \right. \\ &\quad \left. - \frac{eV\Gamma}{2} \arctan\left(\frac{eV}{2\Gamma}\right) \right], \end{aligned} \quad (\text{A4})$$

$$\begin{aligned} \mathcal{S}_{RR}^{eh} &= \frac{e}{h} \text{sign}(V) \left[-\frac{(eV\Gamma)^2}{4[\Gamma^2 + (eV/2)^2]} \right. \\ &\quad \left. + \frac{eV\Gamma}{2} \arctan\left(\frac{eV}{2\Gamma}\right) \right], \end{aligned} \quad (\text{A5})$$

$$\begin{aligned} \mathcal{S}_{LL}^{hh} &= \frac{1}{h} \text{sign}(V) \left[\frac{eV\Gamma^2}{8} \frac{(eV)^2 + 12\Gamma^2}{\Gamma^2 + (eV/2)^2} \right. \\ &\quad \left. + \frac{\Gamma}{4} [(eV)^2 - 12\Gamma^2] \arctan\left(\frac{eV}{2\Gamma}\right) \right], \end{aligned} \quad (\text{A6})$$

$$\mathcal{S}_{RR}^{hh} = \mathcal{S}_{LL}^{hh}, \quad (\text{A7})$$

and for the cross-correlators:

$$\mathcal{S}_{LR}^{ee} = -\mathcal{S}_{LL}^{ee}, \quad (\text{A8})$$

$$\mathcal{S}_{LR}^{he} = -\mathcal{S}_{LL}^{eh}, \quad (\text{A9})$$

$$\mathcal{S}_{LR}^{eh} = -\mathcal{S}_{RR}^{eh}, \quad (\text{A10})$$

$$\begin{aligned} \mathcal{S}_{LR}^{hh} &= -\frac{1}{h} \text{sign}(V) \left[\frac{3\Gamma^2 eV}{2} \right. \\ &\quad \left. - \frac{\Gamma}{4} [(eV)^2 + 12\Gamma^2] \arctan\left(\frac{eV}{2\Gamma}\right) \right]. \end{aligned} \quad (\text{A11})$$

Appendix B: QD currents and noises in the high voltage regime

Performing the integration of Eqs. (5) and (6) at zero temperature for the QD, the currents read as:

$$I_{L,R}^e = \pm \frac{e\Gamma}{h} \sum_{\pm} \left[\pm \arctan\left(\frac{\epsilon_0 \pm eV/2}{\Gamma}\right) \right], \quad (\text{B1})$$

$$\begin{aligned} I_{L,R}^h &= \pm \frac{\Gamma(\epsilon_0 \mp eV/2)}{h} \sum_{\pm} \left[\pm \arctan\left(\frac{\epsilon_0 \pm eV/2}{\Gamma}\right) \right] \\ &\quad \pm \frac{\Gamma^2}{2h} \ln \left[\frac{\Gamma^2 + (\epsilon_0 - eV/2)^2}{\Gamma^2 + (\epsilon_0 + eV/2)^2} \right]. \end{aligned} \quad (\text{B2})$$

In addition, Eqs. (40), (41), (42), (43), (44) and (45) give at zero temperature for the auto-correlators:

$$\begin{aligned} \mathcal{S}_{LL}^{ee} &= \frac{e^2}{h} \text{sign}(V) \sum_{\pm} \left[\pm \frac{\Gamma^2}{2} \frac{\epsilon_0 \mp eV/2}{(\epsilon_0 \mp eV/2)^2 + \Gamma^2} \right. \\ &\quad \left. \mp \frac{\Gamma}{2} \arctan\left(\frac{\epsilon_0 \mp eV/2}{\Gamma}\right) \right], \end{aligned} \quad (\text{B3})$$

$$\begin{aligned} \mathcal{S}_{LL}^{eh} &= \frac{e}{h} \text{sign}(V) \left(\sum_{\pm} \left[\frac{\Gamma^2 eV}{4} \frac{\epsilon_0 \mp eV/2}{(\epsilon_0 \mp eV/2)^2 + \Gamma^2} \right. \right. \\ &\quad \left. \left. \mp \frac{\Gamma \epsilon_0}{2} \arctan\left(\frac{\epsilon_0 \mp eV/2}{\Gamma}\right) \right] \right. \\ &\quad \left. + \frac{\Gamma^2}{2} \ln \left[\frac{\Gamma^2 + (\epsilon_0 - eV/2)^2}{\Gamma^2 + (\epsilon_0 + eV/2)^2} \right] \right) - \frac{V}{2} \mathcal{S}_{LL}^{ee}, \end{aligned} \quad (\text{B4})$$

$$\begin{aligned}
\mathcal{S}_{RR}^{eh} &= \frac{e}{h} \text{sign}(V) \left(\sum_{\pm} \left[\frac{\Gamma^2 eV}{4} \frac{\epsilon_0 \mp eV/2}{(\epsilon_0 \mp eV/2)^2 + \Gamma^2} \right. \right. \\
&\quad \left. \mp \frac{\Gamma \epsilon_0}{2} \arctan \left(\frac{\epsilon_0 \mp eV/2}{\Gamma} \right) \right] \\
&\quad \left. + \frac{\Gamma^2}{2} \ln \left[\frac{\Gamma^2 + (\epsilon_0 - eV/2)^2}{\Gamma^2 + (\epsilon_0 + eV/2)^2} \right] \right) + \frac{V}{2} \mathcal{S}_{RR}^{ee} \quad (\text{B5}) \\
&= \mathcal{S}_{LL}^{eh} + V \mathcal{S}_{LL}^{ee}, \quad (\text{B6})
\end{aligned}$$

$$\begin{aligned}
\mathcal{S}_{LL}^{hh} &= \frac{\text{sign}(V)}{h} \left(\sum_{\pm} \left[\frac{\Gamma^2 eV}{2} \right. \right. \\
&\quad \pm \frac{\Gamma^2}{2} \frac{\epsilon_0^2 (\epsilon_0 \mp eV/2) + \Gamma^2 (\epsilon_0 \pm eV/2)}{(\epsilon_0 \mp eV/2)^2 + \Gamma^2} \\
&\quad \mp \frac{\Gamma(\epsilon_0^2 - 3\Gamma^2)}{2} \arctan \left(\frac{\epsilon_0 \mp eV/2}{\Gamma} \right) \left. \right] \\
&\quad + \Gamma^2 \epsilon_0 \ln \left[\frac{\Gamma^2 + (\epsilon_0 - eV/2)^2}{\Gamma^2 + (\epsilon_0 + eV/2)^2} \right] \\
&\quad - V \mathcal{S}_{LL}^{eh} - \frac{V^2}{4} \mathcal{S}_{LL}^{ee}, \quad (\text{B7})
\end{aligned}$$

$$\begin{aligned}
\mathcal{S}_{RR}^{hh} &= \frac{\text{sign}(V)}{h} \left(\sum_{\pm} \left[\frac{\Gamma^2 eV}{2} \right. \right. \\
&\quad \pm \frac{\Gamma^2}{2} \frac{\epsilon_0^2 (\epsilon_0 \mp eV/2) + \Gamma^2 (\epsilon_0 \pm eV/2)}{(\epsilon_0 \mp eV/2)^2 + \Gamma^2} \\
&\quad \mp \frac{\Gamma(\epsilon_0^2 - 3\Gamma^2)}{2} \arctan \left(\frac{\epsilon_0 \mp eV/2}{\Gamma} \right) \left. \right] \\
&\quad + \Gamma^2 \epsilon_0 \ln \left[\frac{\Gamma^2 + (\epsilon_0 - eV/2)^2}{\Gamma^2 + (\epsilon_0 + eV/2)^2} \right] \\
&\quad + V \mathcal{S}_{RR}^{eh} - \frac{V^2}{4} \mathcal{S}_{RR}^{ee} \quad (\text{B8})
\end{aligned}$$

$$= \mathcal{S}_{LL}^{hh} + 2V \mathcal{S}_{LL}^{eh} + V^2 \mathcal{S}_{LL}^{ee}, \quad (\text{B9})$$

and for the cross-correlators:

$$\mathcal{S}_{LR}^{ee} = -\mathcal{S}_{LL}^{ee}, \quad (\text{B10})$$

$$\mathcal{S}_{LR}^{he} = -\mathcal{S}_{LL}^{eh}, \quad (\text{B11})$$

$$\mathcal{S}_{LR}^{hh} = -\frac{\text{sign}(V)}{h} \left(\sum_{\pm} \left[\frac{\Gamma^2 eV}{2} \right. \right. \quad (\text{B12})$$

$$\begin{aligned}
&\quad \pm \frac{\Gamma^2}{2} \frac{\epsilon_0^2 (\epsilon_0 \mp eV/2) + \Gamma^2 (\epsilon_0 \pm eV/2)}{(\epsilon_0 \mp eV/2)^2 + \Gamma^2} \\
&\quad \mp \frac{\Gamma(\epsilon_0^2 - 3\Gamma^2)}{2} \arctan \left(\frac{\epsilon_0 \mp eV/2}{\Gamma} \right) \left. \right] \\
&\quad + \Gamma^2 \epsilon_0 \ln \left[\frac{\Gamma^2 + (\epsilon_0 - eV/2)^2}{\Gamma^2 + (\epsilon_0 + eV/2)^2} \right] \bigg) - \frac{V^2}{4} \mathcal{S}_{LR}^{ee}. \quad (\text{B13})
\end{aligned}$$

-
- ¹ R. Venkatasubramanian, E. Siivola, T. Colpitts, and B. O'Quinn, *Nature* **413**, 597 (2001).
² T.C. Harman, P.J. Taylor, M.P. Walsh, B.E. Laforge, *Science* **297**, 5590 (2002).
³ P. Reddy, S.-Y. Jang, R.A. Segalman, and A. Majumdar, *Science* **315**, 5818 (2007).
⁴ G.U. Sumanasekera, B.K. Pradhan, H.E. Romero, K.W. Adu, and P.C. Eklund, *Phys. Rev. Lett.* **89**, 166801 (2002).
⁵ J.P. Small, K.M. Perez, and P. Kim, *Phys. Rev. Lett.* **91**, 256801 (2003).
⁶ B. Ludolph and J.M. van Ruitenbeek, *Phys. Rev. B* **59**, 12290 (1999).
⁷ M. Walter, J. Walowski, V. Zbarsky, M. Münzenberg,

- M. Schäfers, D. Ebke, G. Reiss, A. Thomas, P. Peretzki, M. Seibt, J.S. Moodera, M. Czerner, M. Bachmann, and Ch. Heiliger, *Nature. Mater.* **10**, 742 (2011).
⁸ F.L. Bakker, A. Slachter, J.-P. Adam, and B.J. van Wees, *Phys. Rev. Lett.* **105**, 136601 (2010).
⁹ R. Scheibner, H. Buhmann, D. Reuter, M.N. Kiselev, and L.M. Molenkamp, *Phys. Rev. Lett.* **95**, 176602 (2005).
¹⁰ S. Fahlvik Svensson, E.A. Hoffmann, N. Nakpathomkun, P.M. Wu, H.Q. Xu, H.A. Nilsson, D. Sanchez, V. Kashcheyevs, and H. Linke, *New J. Phys.* **15**, 105011 (2013).
¹¹ U. Sivan and Y. Imry, *Phys. Rev. B* **33**, 551 (1986).
¹² P.N. Butcher, *J. Phys.: Condens. Matter* **2**, 4869 (1990).
¹³ J. Azema, A.-M. Daré, S. Schafer, and P. Lombardo, *Phys.*

- Rev. B **86**, 075303 (2012).
- ¹⁴ P. Dutt and K. Le Hur, Phys. Rev. B **88**, 235133 (2013).
 - ¹⁵ K.A. Matveev and A.V. Andreev, Phys. Rev. B **66**, 045301 (2002).
 - ¹⁶ O. Entin-Wohlman, Y. Imry, and A. Aharony, Phys. Rev. B **82**, 115314 (2010).
 - ¹⁷ A. Crépieux, F. Simkovic, B. Cambon, and F. Michelini, Phys. Rev. B **83**, 153417 (2011).
 - ¹⁸ L. Arrachea, M. Moskalets, and L. Martin-Moreno, Phys. Rev. B **75**, 245420 (2007).
 - ¹⁹ E. Iyoda, Y. Utsumi, and T. Kato, J. Phys. Soc. Jpn. **79**, 045003 (2010).
 - ²⁰ M.G. Vavilov and A.D. Stone, Phys. Rev. B **72**, 205107 (2005).
 - ²¹ Y. Dubi and M. Di Ventra, Nano Lett. **9**, 97 (2009).
 - ²² J. Matthews, F. Battista, D. Sanchez, P. Samuelsson, and H. Linke, arXiv:1306.3694 (2013).
 - ²³ B. Muralidharan and M. Grifoni, Phys. Rev. B **85**, 155423 (2012).
 - ²⁴ R.S. Whitney, Phys. Rev. B **88**, 064302 (2013).
 - ²⁵ R.S. Whitney, Phys. Rev. Lett. **112**, 130601 (2014).
 - ²⁶ D.M. Kennes, D. Schuricht, and V. Meden, Europhys. Lett. **102**, 57003 (2013).
 - ²⁷ I.V. Krive, E.N. Bogachek, A.G. Scherbakov, and U. Landman, Phys. Rev. B **64**, 233304 (2001).
 - ²⁸ M. Kindermann and S. Pilgram, Phys. Rev. B **69**, 155334 (2004).
 - ²⁹ F. Zhan, S. Denisov, and P. Hänggi, Phys. Rev. B **84**, 195117 (2011).
 - ³⁰ F. Battista, M. Moskalets, M. Albert, and P. Samuelsson, Phys. Rev. Lett. **110**, 126602 (2013).
 - ³¹ M. Moskalets, arXiv:1402.1050 (2014).
 - ³² F. Giazotto, T.T. Heikkila, A. Luukanen, A.M. Savin, and J.P. Pekola, Rev. Mod. Phys. **78**, 217 (2006).
 - ³³ R. Sanchez, B. Sothmann, A.N. Jordan, and M. Büttiker, New J. Phys. **15**, 125001 (2013).
 - ³⁴ Ya.M. Blanter and M. Büttiker, Phys. Rep. **336**, 1 (2000).
 - ³⁵ M. Apostol, J. Appl. Phys. **104**, 053704 (2008).
 - ³⁶ M. Kindermann and Yu.V. Nazarov, Phys. Rev. Lett. **91**, 136802 (2003).
 - ³⁷ I. Safi and H. Saleur, Phys. Rev. Lett. **93**, 126602 (2004).
 - ³⁸ R. Zamoum, A. Crépieux, and I. Safi, Phys. Rev. B **85**, 125421 (2012).
 - ³⁹ F.D. Parmentier, A. Anthore, S. Jezouin, H. le Sueur, U. Gennser, A. Cavanna, D. Mailly, and F. Pierre, Nature Physics **7**, 935 (2011).
 - ⁴⁰ C. de C. Chamon, D.E. Freed, and X.G. Wen, Phys. Rev. B **53**, 4033 (1996).
 - ⁴¹ J. von Delft, H. Schoeller, Ann. Phys. **7**, 225 (1998).
 - ⁴² S. Jezouin, F.D. Parmentier, A. Anthore, U. Gennser, A. Cavanna, Y. Jin, and F. Pierre, Science **342**, 601-604 (2013).
 - ⁴³ C.L. Kane and M.P.A. Fisher, Phys. Rev. B **46**, 15233 (1992); C.L. Kane and M.P.A. Fisher, Phys. Rev. Lett. **68**, 1220 (1992); T. Giamarchi and H.J. Schulz, Phys. Rev. B **37**, 325 (1988).
 - ⁴⁴ M. Paulsson and S. Datta, Phys. Rev. B **67**, R241403 (2003).